LEVEL SET SEGMENTATION OF SPINAL VERTEBRAE

V.Malathy , Jaya Engineering College
malathyvanniappan@gmail.com
Dr.S.Nirmala
Assistant Professor, ECE Department
Jaya Engineering College
9677143219

Abstract: **Segmentation of spinal vertebrae in 3-D space is a crucial step in the study of spinal related disease or disorders. However, the complexity of vertebrae shapes, with gaps in the cortical bone and boundaries, as well as noise, in homogeneity, and incomplete information in images, has made spinal vertebrae segmentation a difficult task. In this paper, we introduce a new method for an accurate spinal vertebrae segmentation that is capable of dealing with noisy images with missing information. This is achieved by introducing an edge-mounted Willmore flow, as well as a prior shape kernel density estimator, to the level set segmentation framework. While the prior shape model provides much needed prior knowledge when information is missing from the image, and draws the level set function toward prior shapes, the edge-mounted Willmore flow helps to capture the local geometry and smoothes the evolving level set surface. Evaluation of the segmentation results with ground-truth validation**
demonstrates the effectiveness of the proposed approach: an overall accuracy of 89.32 ± 1.70% and 14.03 ± 1.40 mm are achieved based on the Dice similarity coefficient and Hausdorff distance, respectively, while the inter- and intra observer variation agreements are 92.11 ± 1.97%, 94.94 ± 1.69%, 3.32 ± 0.46, and 3.80 ± 0.56 mm.

I .INTRODUCTION

Spine trauma is a devastating event with high morbidity and mortality, causing severe psychological, social, and financial burdens for patients, their families, and the society. Among the spine trauma incidents, motor vehicle accidents account for 42.1% of reported spinal cord injury cases, followed by falls (26.7%), acts of violence (15.1%) and sporting activities v (7.6%). Compression fractures of the vertebral body in older adults are common, due to osteoporosis. Fractures of the thoracic and lumbar spine are more widespread than of the cervical spine, with highly affected area in thoracolumbar region (T11 to L4). Fractures and dislocations of spine may give rise to potentially devastating long-term consequences such as neural deficits, permanent disability, or even death. Fig. 1 shows examples of spinal disorders due to trauma and osteoporosis in computed tomography (CT) images. Identifying and grading severity of spine fractures and understanding their cause will help physicians determine the most effective pharmacological treatments and clinical management strategies for spinal disorders. One of the major challenges is to achieve *a firm diagnosis*. Detection and segmentation of spine from images are crucial steps in diagnostic imaging. Although these quantitative image analysis techniques have received increasing interest, accurate detection and segmentation methods are still lacking. Spine segmentation remains challenging due to the complexity of vertebrae shapes, gaps in the cortical bone and boundaries, as well as noise, inhomogeneity, and incomplete information in images, as shown in Fig. 2.

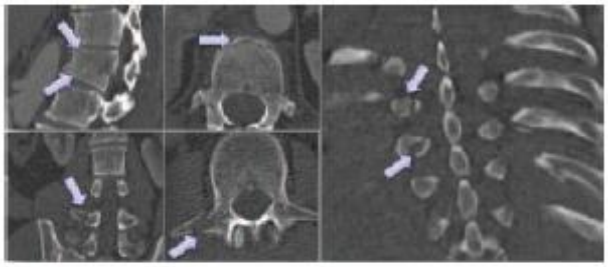

Fig. 1. Fractures of the vertebrae are indicated by arrows.

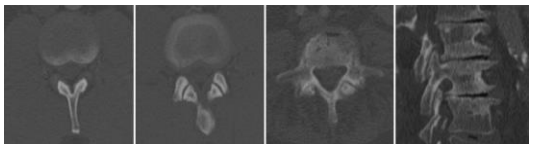

Fig. 2. Incomplete, missing or ambiguous information of the vertebrae in CT images.

II. VERTEBRA SEGMENTATION

A.Level Set

The level set method, also known as the implicit deformable model, embeds an interface in a higher dimensional function φ (the signed distance function) as a level set $\varphi = 0$. The equation that governs the evolution of the level set function $\varphi(t)$ is $\partial\varphi/\partial t + F|\nabla\varphi| = 0$, where F is the speed function. The level set method has been widely used for image segmentation. Recent developments of the methods however have largely focused on the variational framework. With this approach, an energy function $E(\varphi)$ is defined in relation to the the speed function. The minimization of such energy generates the Euler-Lagrange equation, and the evolution of the equation is through calculus of variation:

$$\frac{\partial\phi}{\partial t} = -\frac{\partial E(\phi)}{\partial\phi}$$

In this paper, we consider the fusion of energies, i.e., using a shape prior distribution estimator Es with an edge-mounted Willmore energy $Ew0$:

$$E(\varphi) = E_s + E_{w0}\ .$$

In order to incorporate a given prior data set $\{\varphi 1, \varphi 2, \ldots, \varphi N\}$ into the level set segmentation framework, we adopt a shape dissimilarity measure based on the kernel density estimation. This non-parametric distribution estimator overcomes two common shortcomings: (1) the assumption that the shapes are Gaussian distributed, which is generally inappropriate; (2) the shapes are represented by signed distance functions, which constitute a nonlinear space that does not include the mean.

A. *Kernel Density Estimation*

Kernel density estimation provides a fundamental smoothing estimator even with a small number of data samples. For N samples of shape models, the density estimation can be formulated as a sum of Gaussian of shape dissimilarity measures
$d^2(H(\varphi),H(\varphi i))$, $i = 1, 2, \ldots, N$:

$$P(\phi) \propto \frac{1}{N}\sum_{i=1}^{N} e^{-\frac{d^2(H(\phi),H(\phi_i))}{2\sigma^2}},$$

where $H(\varphi)$ is the *Heaviside* function and

$$d^2(H(\phi),H(\phi_i)) = \int_\Omega \frac{1}{2}\left(H(\phi) - H(\phi_m)\right)^2 dx,$$

$$\sigma^2 = \frac{1}{N}\sum_{i=1}^{N} \min_{j\neq i} d^2(H(\phi_i),H(\phi_j)).$$

The segmentation is obtained by maximizing the conditional probability of φ given image intensity I:

$$P(\phi|I) = \frac{P(I|\phi)P(\phi)}{P(I)}$$

By considering the shape energy as
$E_s(\varphi) = -\log P(\varphi|I)$,
the variational with respect to φ becomes

$$\begin{aligned}\frac{\partial E_s}{\partial\phi} &= \frac{\sum_{i-1}^{N}\alpha_i\frac{\partial}{\partial\phi}d^2(H\phi,H\phi_i)}{2\sigma^2\sum_{i-1}^{N}\alpha_i}\\ &= \sum_{i-1}^{N}\frac{e^{-\frac{d^2(H\phi,H\phi_i)}{2\sigma^2}}}{2\sigma^2\sum_{i-1}^{N}\alpha_i}\left(2\delta(\phi)\left[H(\phi) - H(\phi_i(x-\mu_\phi))\right]\right.\\ &\quad + \int\left[H(\phi(\xi) - H(\phi_i(\xi-\mu_\phi))\right]\\ &\quad \left.\delta\phi(\xi)\frac{(x-\mu_\phi)^T\nabla\phi(\xi)}{\int H\phi dx}d\xi\right),\end{aligned}$$

where μ_φ is the centroid of φ and $\alpha_i = \exp\left(-\frac{1}{2\sigma^2}d^2(H\phi,H\phi_i)\right)$
is the weight factor for $i = 1, 2, \ldots, N$.

B. *Willmore Flow*

The Willmore flow is a function of mean curvature capturing the deviation of a surface from (local) sphericity. The associated energy function is formulated as

$$E_w = \frac{1}{2}\int_M h^2 dA,$$

where M is a d-dimensional surface embedded in R^{d+1} and h the mean curvature on M.
As a geometric functional, the Willmore energy is defined on the geometric representation of a collection of level sets. Its gradient flow can be well represented by defining a suitable metric, the Frobenius norm, on the space of the level sets. Frobenius norm is a convenient choice as it is equivalent to the $l2$-norm of a matrix and more importantly it is computationally attainable. As Frobenius norm is an inner-product norm, the optimization in the variational method comes naturally. Based on the formulation by Droske and Rumpf, the Willmore flow or the variational form for the Willmore energy with respect to φ is

$$\frac{\partial E_w}{\partial\phi} = -\|\nabla\phi\|\left(\Delta_M h + h(t)\left(\|S(t)\|_2^2 - \frac{1}{2}h(t)^2\right)\right)$$

Where
$\Delta_M h = \Delta h - h\frac{\partial h}{\partial n} - \frac{\partial^2 h}{\partial n^2}$
is the Laplacian Beltrami operator on h with

$$n = \frac{\nabla\phi}{\|\nabla\phi\|},\ S = (I - n\otimes n)(\nabla\times\nabla)\phi$$

is the shape operator on φ and
$\|S\|_2$ is the Frobenius norm of S.
In order to ensure the smoothing effect by Willmore energy work nicely around the constructed surface and not affecting

the desired edge of vertebrae, we propose to multiply the edge indicator function $g(I)$ with Willmore flow:

$$\frac{\partial E_{w_0}}{\partial \phi} = -g(I)\|\nabla\phi\|\left(\Delta_M h + h(t)\left(\|S(t)\|_2^2 - \frac{1}{2}h(t)^2\right)\right),$$

where

$$g(I) = \frac{1}{1+|\nabla G_\sigma * I|^2}$$

G_σ is the Gaussian filter with standard deviation σ.

III.EXPERIMENTAL RESULTS

A..Clinical Data and Ground-Truth Construction

The dataset consists of 20 CT images of normal spinal vertebrae images of patients aged 18 to 66. The patients are carefully selected by radiologists to form a representative group. These images are acquired from various CT scanners such as 32- detector row Siemens definition, 64-detector row Philips Brilliance, and 320-detector row Toshiba Aquilion. The in-plane resolutions for these images range from 0.88 to 1.14 mm, with consistent slice thickness of 2 mm. Original images have fixed sizes
of 512 × 512, with slices varying from 45 to 98. The ground truths are obtained by manual delineations using TURTLESEG, an interactive 3-D image segmentation software and verified by radiologists. Although 3-D manual delineation is time consuming, the benefits are twofold: 1) it allows validation of segmentation results; 2) it serves as shape models in the segmentation framework. With a torus as the initial contour set manually, the level set method is implemented around a narrow band with reinitialization algorithm. The classical Caselles and Chan–Vese models are combined with prior shape energies to obtain various segmentation results. The popular segmentation methods such as graph cut and region growing are used for comparison with the proposed method. The inter- and intra observer variation estimation for manual delineations of ground truths are acquired to verify the difficulty of segmentation tasks in 3-D using the dataset. The leave-one-out approach is applied for cross validation and results are validated with the ground truth.

B.. Segmentation Results and Comparisons

First, we compare the segmentation results obtained by the classical level set model driven by mean curvature flow as proposed by Caselles and level set evolution using the edge mounted Willmore energy. The Caselles energy fails to fully segment the spinal canal since partial edge information is missing. It is that the Willmore energy maintains steady flow from initial contour with smooth level set evolution. However, this evolution is highly dependent on the initial contour, thus the segmentation must be accomplished with proper guidance to achieve desired results. For example, with the edge-mounted Willmore energy, segmentation clearly moves toward the spinal canal. The results show that Chan–Vese energy suffers from edge leaking to other vertebras, and the approaches fail to capture the full vertebrae shape when image inhomogeneity is present. The leaking problem is not resolved even when Chan–Vese energy is combined with shape prior energy, since the nearby vertebras are closely connected and share similar image intensities. Similarly, the leaking problem happens when the Caselles model is used due to incomplete edges in the image, and adding prior shape energy does not help the situation. The region growing algorithm fails to segment the vertebrae, and the graph-cut algorithm suffers badly from leaking.The edge-mounted Willmore energy is able to overcome problems such as incomplete edges and leaking, with added advantage of smoothing the segmentation. However, it can be halted by noisy patches before reaching the edges. Thus, a prior shape energy is incorporated to resolve the problem. The vertebrae shape is completely captured by the proposed framework.

C.Quantitative Evaluation of Segmentation

The Dice similarity coefficient (DSC) and Hausdorff distance (HD) are used to measure the intrinsic index of segmentation performance. While DSC measures the relative superposition between two enclosed volumes, HD measures the relative differences between boundaries of the segmented objects.
The DSC is formulated as

$$D(\Omega_S, \Omega_G) = \frac{2(|\Omega_S \bigcap \Omega_G|)}{|\Omega_S| + |\Omega_G|}$$

where $|\Omega S|$ and $|\Omega G|$ represent the volumes of segmented object ΩS and the ground-truth ΩG, respectively. The measurement (varies from 0 to 1) indicates the correspondence between two volumes, i.e., 0 means the two volumes do not overlap and 1 shows they are perfectly matched. On the other hand, the HD is defined as

$$d_H(X,Y) = \max\{\sup_{x\in X}\inf_{y\in Y} d(x,y), \sup_{y\in Y}\inf_{x\in X} d(x,y)\}$$

where X and Y are the boundaries of two different segmented volumes, respectively. It measures the distance between the farthest point of a set to the nearest point of the other and vice versa. The measurement (varies from 0 to ∞ theoretically) signifies the difference between two closed surfaces, e.g., 0 indicates that both volumes share exactly the same boundaries, and larger HD values mean larger distances between the boundaries. In summary, a high DSC and a low HD are desirable for good segmentation. In this study, the DSC are converted into 100 percentile for general physical interpretation.

Even without integrating prior shape into the segmentation framework, the edge-mounted Willmore flow leads to superior segmentation results (DSC 75.82 ± 2.81%, HD19.26 ± 1.51 mm) over other methods, e.g., Caselle swith prior shape models (DSC 71.12 ± 2.72%, HD 18.39 ± 1.15 mm), Chan–Vese with prior shape models (45.09 ± 7.54%, HD 25.31 ± 2.38 mm), region growing (DSC 42.30 ± 11.43%, HD 25.20 ± 2.30 mm), graph cut (DSC 13.23 ± 11.11%, HD 63.37 ± 14.42 mm), as well as Caselles and Chan–Vese models without prior shape models. By integrating both edge-mounted Willmore flow and prior shape models, the proposed approach has achieved an overall accuracy of 89.32 ± 1.70% (DSC) and 14.03 ± 1.40 mm (HD), clearly outperforming the other methods. The level of difficulty of the segmentation tasks on the dataset is determined by inter- and intra observer agreements. For an inter observer agreement, manual delineation on the same dataset is performed by two independent observers. Whereas for an intra observer agreement, two manual delineations are performed by an observer, with the second annotation done one week after the first. Based on the DSC and HD evaluation schemes, the inter- and intra observer agreements for the dataset are 92.11 ± 1.97%, 94.94 ± 1.69% (DSC), 3.32 ± 0.46 mm, and 3.80 ± 0.56 mm (HD), respectively.

C. Computational Complexity Analysis

The experimental results in Section V show that the performance of our algorithm is superior in terms of accuracy over others such as region-growing and graph-cut algorithms. This improvement in accuracy, however, introduces an increased computational cost. The complexity of our algorithm is $O(N2)$, where N is the image size. This is comparable to that of the algorithm proposed by Cremer *et al.* The computational cost is related to the number of operators involved in the algorithm. As the gradient descent evolution algorithm is governed by a combination of regional difference, dissimilarity measure and Willmore energy, the number of operators increases accordingly. The main advantage of our algorithm is its accuracy segmenting highly complex anatomical objects.

IV.CONCLUSION AND FUTURE WORK

We have presented a new segmentation framework based on the level set for spinal vertebrae segmentation. The framework incorporates not only prior shape knowledge through the KDE method, but also local geometrical features through Willmore flow, into the level set segmentation. Experimental results on CT images, validated with ground truth, demonstrate the effectiveness of proposed framework. The framework has achieved much higher segmentation accuracy than existing methods, such as Chan–Vese and Caselles, region growing, and graph cut. Ongoing research includes integrating the segmentation framework into a system for detection and quantification of vertebrae fractures and other diseases of the spine.

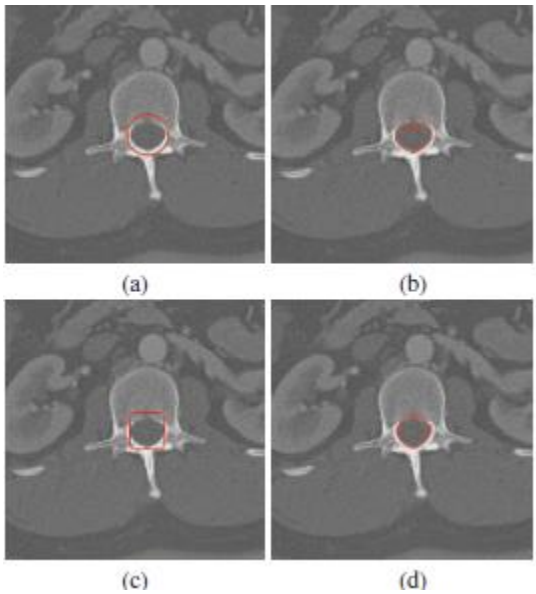

Fig. 2. (a) Initial contour. Segmented samples obtained by (b) Caselles, (c) Willmore, (d) edge mounted Willmore approach

REFERENCES

[1] S. Looby and A. Flanders. (2011, Jan.). Spine trauma. *Radiol. Clin. North. Am.* [Online]. *49(1)*, pp. 129–163, Available:http://linkinghub.elsevier.com/retrieve/pii/S0033838910001454

[2] B. Naegel, "Using mathematical morphology for the anatomical labeling of vertebrae from 3-D CT-scan images," *Comput. Med. Imaging Grap.*, vol. 31, no. 3, pp. 141–156, 2007.

[3] S. Ghebreab and A. Smeulders. (2004, Oct.). Combining strings and necklaces for interactive three-dimensional segmentation of spinal images using an integral deformable spine model. *IEEE Trans. Biomed. Eng.* [Online]. *51(10)*, pp. 1821–1829, Available: http://ieeexplore.ieee.org/lpdocs/epic03/wrapper.htm?arnumber=1337150

[4] J.Ma, L. Lu, Y. Zhan, X. Zhou, M. Salganicoff, and A. Krishnan, "Hierarchical segmentation and identification of thoracic vertebra using learningbased edge detection and coarse-to-fine deformable model," in *Proc. Int. Conf. Med. Imag. Comput. Comput. Aided Intervention*, 2010, pp. 19–27.

[5] C. Lorenz and N. Krahnstoever, "3D statistical shape models for medical image segmentation," in *Proc. 2nd Int. Conf. 3-D Dig. Imag.Model.*, 1999, pp. 4–8.

[6] T. Klinder, J. Ostermann, M. Ehm, A. Franz, R. Kneser, and C. Lorenz. (2009, Jun.). Automated model-based vertebra detection, identification, and segmentation in ct images. *Med. Imag. Anal.* [Online]. *13(3)*, pp. 471–482, Available: http://linkinghub.elsevier.com/retrieve/pii/ S1361841509000085

[7] A. Mastmeyer, K. Engelke, C. Fuchs, andW. A. Kalender, "A hierarchical 3-d segmentation method and the definition of vertebral body coordinate systems for qct of the lumbar spine," *Med. Image Anal.*, vol. 10, pp. 560– 577, 2006.